

**M. L. Rodrigues,^a
 M. J. Bonifácio,^b P. Soares-da-
 Silva,^b ‡ M. A. Carrondo^a and
 M. Archer^{a*}**

^aInstituto de Tecnologia Química e Biológica (ITQB), Universidade Nova de Lisboa, Av. República, Apt. 127, 2781-901 Oeiras, Portugal, and ^bDepartment of Research and Development, BIAL, 4785 S. Mamede do Coronado, Portugal

‡ Permanent address: Institute of Pharmacology and Therapeutics, Faculty of Medicine, 4200 Porto, Portugal.

Correspondence e-mail: archer@itqb.unl.pt

Received 17 September 2004

Accepted 26 November 2004

Online 24 December 2004

Crystallization and preliminary X-ray diffraction studies of a catechol-*O*-methyltransferase/inhibitor complex

Inhibitors of the enzyme catechol-*O*-methyltransferase (COMT) are used as co-adjuvants in the therapy of Parkinson's disease. A recombinant form of the soluble cytosolic COMT from rat has been co-crystallized with a new potent inhibitor, BIA 8-176 [(3,4-dihydroxy-2-nitrophenyl)phenylmethanone], by the vapour-diffusion method using PEG 6K as precipitant. Crystals diffract to 1.6 Å resolution on a synchrotron-radiation source and belong to the monoclinic space group *P*2₁, with unit-cell parameters $a = 52.77$, $b = 79.63$, $c = 61.54$ Å, $\beta = 91.14^\circ$.

1. Introduction

Catechol-*O*-methyltransferase (COMT; EC 2.1.1.6) is an enzyme that plays an important role in the metabolism of biologically active compounds and in the detoxification of xenobiotics containing a catechol moiety (Mannisto & Kaakkola, 1999). The enzyme catalyses the transfer of a methyl group from *S*-adenosylmethionine (SAM) to a hydroxyl O atom of the catechol in the presence of an Mg²⁺ ion (Axelrod & Tomchick, 1958; Guldberg & Marsden, 1975). Physiological COMT substrates include catecholamine neurotransmitters (adrenaline, noradrenaline and dopamine; Axelrod & Tomchick, 1958), catechol oestrogens (Creveling *et al.*, 1970) and ascorbic acid (Blaschke & Hertting, 1971). Although COMT is an ubiquitous protein in nature, it has been extensively studied in mammals, where it is present in most tissues (Guldberg & Marsden, 1975; Karhunen *et al.*, 1994; Lundstrom *et al.*, 1995). There are two forms of COMT: a soluble cytosolic protein (S-COMT) and a membrane-bound protein (MB-COMT; Assicot & Bohuon, 1971; Roth, 1992), which is anchored to rough endoplasmic reticulum by a transmembrane peptide (Lundstrom *et al.*, 1995; Vidgren *et al.*, 1999) and whose soluble part is facing the cytoplasm. Both proteins are coded by a single gene using different promoters (Lundstrom *et al.*, 1991; Tenhunen *et al.*, 1993). Rat and human S-COMT have 221 amino-acid residues and show 81% sequence identity. MB-COMT proteins have additional N-terminal extensions of 43 and 50 amino acids in rats and humans, respectively (Lotta *et al.*, 1995; Lundstrom *et al.*, 1995).

Parkinson's disease (PD) results from a slowly progressive loss of dopaminergic neurons and is one of the most common neurodegenerative disorders in the elderly (Dawson & Dawson, 2003). Although some insights into the molecular mechanisms in PD have recently been reported (Greenamyre & Hastings, 2004), there are not yet any neuroprotective or neurorestorative therapies. The most effective symptomatic therapy has been dopamine replacement in the brain by administration of its precursor, L-dopa, in conjunction with a peripheral aromatic L-amino-acid decarboxylase (AADC) inhibitor. However, under AADC inhibition most L-dopa is inactivated by COMT before it reaches the brain, resulting in a very low drug bioavailability. Therefore, a COMT inhibitor is used as co-adjuvant in the treatment of PD. Since the late 1980s, several highly potent and selective COMT inhibitors sharing a nitrocatechol structure have been developed (Mannisto *et al.*, 1988; Zurcher *et al.*, 1990). It has been shown that these inhibitors significantly enhance the efficacy of PD therapy by increasing the L-dopa half-life (Bonifati & Meco, 1999; Olanow & Stocchi, 2004).

The three-dimensional structure of S-COMT in complex with the inhibitor 3,5-dinitrocatechol and the cosubstrate SAM was first described by Vidgren *et al.* (1994), opening new perspectives for



© 2005 International Union of Crystallography
 All rights reserved

rational drug design (Masjost *et al.*, 2000; Vidgren, 1998). More recently, two other structures of S-COMT have been determined, one in complex with a bisubstrate inhibitor (Lerner *et al.*, 2001), where both substrate and cosubstrate analogues are covalently linked, and the other in complex with SAM and a new tight-binding inhibitor, BIA 3-335 (Bonifacio *et al.*, 2002). This structure shows that large substituents (*R* groups) of the inhibitor extend out of the active-site cavity towards the solvent, with higher thermal factors than the nitrocatechol moiety responsible for anchoring the inhibitor to the enzyme.

In this report, we describe the crystallization and preliminary crystallographic data of recombinant rat S-COMT complexed with cosubstrate SAM and a potent and reversible inhibitor BIA 8-176 [(3,4-dihydroxy-2-nitrophenyl)phenylmethanone] with possible therapeutic applications. The crystals of this complex are not isomorphous to those of BIA 3-335, possibly owing to modifications of crystal contacts induced by the nature and size of the inhibitor *R* group. BIA 8-176 is a novel inhibitor that acts both in the peripheral and the central nervous system. We aim towards a detailed structural characterization of the molecular interactions of the enzyme S-COMT with different inhibitors.

2. Experimental

2.1. Protein expression and purification

Recombinant rat S-COMT was produced in *Escherichia coli* in fusion with the calmodulin-binding peptide tag, which was removed by enterokinase digestion as described previously (Bonifacio *et al.*, 2001). The purity of the protein sample was assessed by electrophoretic and dynamic light-scattering analysis.

2.2. Crystallization

The protein was concentrated to 14 mg ml⁻¹ using an Amicon diaflow device with a YM10 ultrafiltration membrane in 10 mM MES pH 6.5, 2.5 mM MgCl₂, 1 mM DTT as buffer. S-COMT was incubated in ice with SAM and BIA 8-176 at 3 and 1.5 molar ratios, respectively. Since BIA 8-176 is insoluble in water, DMSO and ethanol were used in equal volumes to prepare the concentrated inhibitor solution. The final concentration of DMSO and ethanol on the COMT complex solution is around 2% (v/v) for each solvent. A similar procedure was used for BIA 3-335 (Rodrigues *et al.*, 2001).

Crystallization experiments were performed by the sitting-drop vapour-diffusion method at 277 and 293 K. Each drop contained equal volumes (2 µl) of protein and reservoir solutions and equilibration was performed against 0.7 ml of reservoir solution. Initial

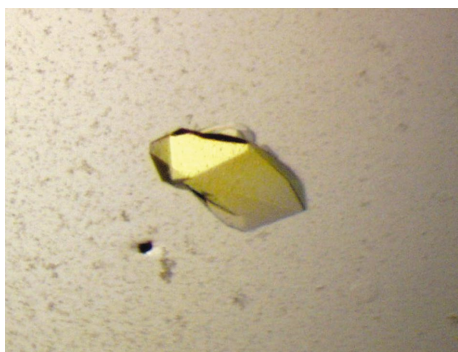


Figure 1
Crystal of the recombinant S-COMT complexed with its cosubstrate, SAM, and the yellow inhibitor BIA 8-176. Its largest dimension is approximately 0.2 mm.

Table 1

X-ray diffraction data for the S-COMT-SAM-BIA 8-176 complex.

Values in parentheses refer to the highest resolution shell (1.64–1.60 Å).

X-ray source	ESRF, ID14-4 beamline
Wavelength (Å)	0.933
Detector	ADSC Quantum 4 CCD
Space group	<i>P</i> 2 ₁
Unit-cell parameters (Å, °)	<i>a</i> = 52.77, <i>b</i> = 79.63, <i>c</i> = 61.54, β = 91.14
No. molecules in AU	2
Resolution range (Å)	24.42–1.60
Mosaicity (°)	0.45
No. unique reflections	67299
Average redundancy	3.5
Completeness (%)	99.9 (98.2)
<i>I</i> /σ(<i>I</i>)	21.6 (3.2)
<i>R</i> _{merge} † (%)	5.4 (39.8)
<i>R</i> _{r.i.m.} † (%)	6.3 (46.9)
<i>R</i> _{p.i.m.} † (%)	3.4 (26.2)

† As defined by Weiss (2001), $R_{\text{merge}} = \frac{\sum_{hkl} \sum_i |I_i(hkl) - \overline{I(hkl)}|}{\sum_{hkl} \sum_i I_i(hkl)}$, $R_{\text{r.i.m.}} = \frac{\sum_{hkl} [N/(N-1)]^{1/2} \sum_i |I_i(hkl) - \overline{I(hkl)}|}{\sum_{hkl} \sum_i I_i(hkl)}$, $R_{\text{p.i.m.}} = \frac{\sum_{hkl} [1/(N-1)]^{1/2} \sum_i |I_i(hkl) - \overline{I(hkl)}|}{\sum_{hkl} \sum_i I_i(hkl)}$.

searches for crystallization conditions were based on those suitable for the crystal growth of the ternary complex S-COMT-SAM-BIA 3-335 (Rodrigues *et al.*, 2001). Structure Screen I from Molecular Dimensions was also utilized to search for further crystallization conditions. The best crystals appeared within 3–5 d in drops containing 2 µl protein solution and 4 µl reservoir solution (8% PEG 6K, 0.1 M MES pH 6.0) and grew to approximate dimensions of 0.20 × 0.15 × 0.10 mm (Fig. 1).

2.3. Data collection and processing

X-ray diffraction data were collected to 1.6 Å resolution from a frozen crystal using an ADSC Quantum 4 CCD detector at the ID14-4 beamline at ESRF, Grenoble. For cryoprotection, the crystal

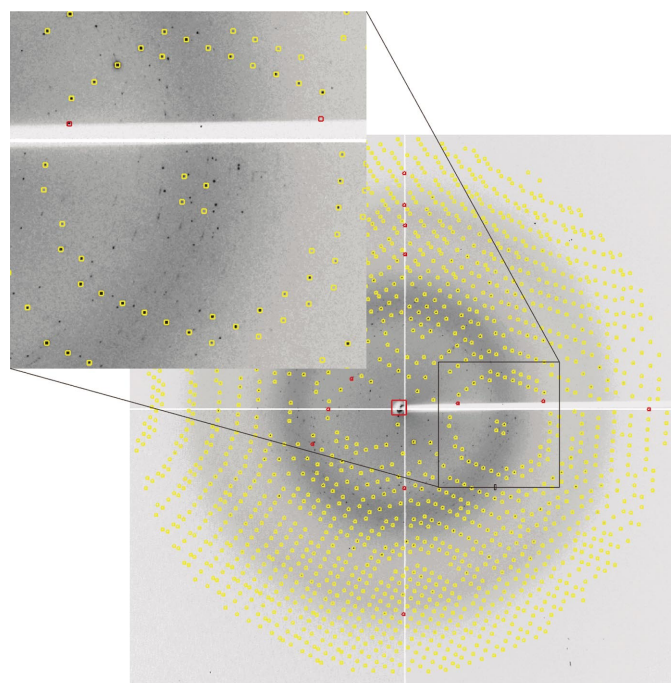


Figure 2
An X-ray diffraction image (0.5° oscillation) of an S-COMT-SAM-BIA 8-176 complex crystal. A close-up view shows the presence of spots that do not belong to the main crystal lattice.

was quickly soaked in the crystallization buffer containing 20% 2,3-butanediol and immediately frozen in liquid nitrogen.

Despite the multiple diffraction pattern (Fig. 2), it was still possible to isolate the main crystal lattice, so the data were processed and integrated using the *HKL* suite of programs (Otwinowski & Minor, 1997) with an R_{merge} of 5.4%. The crystal belongs to the monoclinic space group $P2_1$, with unit-cell parameters $a = 52.77$, $b = 79.63$, $c = 61.54$ Å, $\beta = 91.14^\circ$. A summary of the data-collection and processing statistics is shown in Table 1. Another data set collected in-house from a crystal mounted on a quartz capillary, which diffracted to 2.8 Å resolution, showed similar unit-cell parameters ($a = 54.14$, $b = 78.13$, $c = 61.07$ Å, $\beta = 91.09^\circ$).

2.4. Structure determination

The structure was solved by the molecular-replacement (MR) method using S-COMT coordinates from the complex with the inhibitor BIA 3-335 (PDB code 1h1d) as a search model. Cosubstrate, inhibitor and solvent molecules were removed prior to the MR procedure. Using reflections in the 15–3.5 Å resolution range, the *AMoRe* program (Navaza, 1994) was able to find the correct solution for both molecules present in the asymmetric unit. After rigid-body refinement, the first solution exhibited a correlation coefficient of 61.2% and an R factor of 35.9%, while the second solution showed a correlation coefficient and an R factor of 33.3 and 46.1%, respectively.

3. Results and discussion

The ternary complex S-COMT–SAM–BIA 8-176 crystallized under similar conditions (8% PEG 6K, 0.1 M MES pH 6.0) as the complex S-COMT–SAM–BIA 3-335. However, the crystal growth is highly dependent on the inhibitor used for co-crystallization. Indeed, we were unable to crystallize S-COMT alone or in complex with several other inhibitor compounds. Crystals with BIA 8-176 frequently showed multiple growth and were not always reproducible. These crystals were also sensitive to changes in mother-liquor solution, with a tendency to degrade or crack upon addition of harvesting buffer or cryoprotecting solutions. Several conditions were used to attempt to cryoprotect the crystals upon freezing. A complete data set was measured at 1.6 Å resolution using synchrotron radiation from a crystal of $\sim 0.20 \times 0.15 \times 0.10$ mm cryoprotected with 20% 2,3-butanediol. Although the diffraction pattern showed some multiplicity (Fig. 2), it was still possible to index the main crystal lattice and to integrate the reflections with an R_{merge} of 5.4%. Reasonable values of the Matthews coefficient ($2.6 \text{ \AA}^3 \text{ Da}^{-1}$) and solvent content (52.6%) are obtained assuming the presence of a dimer in the asymmetric unit (Matthews, 1968). A self-rotation function calculated using the program *POLARRFN* from the *CCP4* package (Collaborative Computational Project, Number 4, 1994) identified a twofold non-crystallographic axis. Since the complex of S-COMT with BIA 8-176 is not isomorphous to the complex of S-COMT with BIA 3-335 (PDB code 1h1d), which belong to the trigonal space group $P3_221$, the structure was solved by the molecular-replacement method using the *AMoRe* program (Navaza, 1994). The three previously determined crystal structures of S-COMT complexes belong to the same trigonal space group ($P3_221$) with one molecule in the asymmetric unit. Their structural comparison shows

that the crystal packing was not significantly affected by the inhibitor used, even though the three inhibitors were quite different. In the present case, S-COMT crystallized in a different space group ($P2_1$) with two molecules in the asymmetric unit. Preliminary difference maps show the inhibitor molecules from both complexes are located on the dimer interface in direct contact with each other. Model fitting and further refinement are in progress.

The authors gratefully acknowledge financial support from Fundação para a Ciência e Tecnologia for research project POCTI/BME/38306/2001 and grant SFRH/BD/5228/2001 (to MLR). We also thank Pedro Matias for X-ray diffraction data collection at the ESRF.

References

- Assicot, M. & Bohuon, C. (1971). *Biochimie*, **53**, 871–874.
- Axelrod, J. & Tomchick, R. (1958). *J. Biol. Chem.* **233**, 702–705.
- Blaschke, E. & Hertzting, G. (1971). *Biochem. Pharmacol.* **20**, 1363–1370.
- Bonifacio, M. J., Archer, M., Rodrigues, M. L., Matias, P. M., Learmonth, D. A., Carrondo, M. A. & Soares-Da-Silva, P. (2002). *Mol. Pharmacol.* **62**, 795–805.
- Bonifacio, M. J., Vieira-Coelho, M. A. & Soares-da-Silva, P. (2001). *Protein Expr. Purif.* **23**, 106–112.
- Bonifati, V. & Meco, G. (1999). *Pharmacol. Ther.* **81**, 1–36.
- Collaborative Computational Project, Number 4 (1994). *Acta Cryst.* **D50**, 760–763.
- Creveling, C. R., Dalgard, N., Shimizu, H. & Daly, J. W. (1970). *Mol. Pharmacol.* **6**, 691–696.
- Dawson, T. M. & Dawson, V. L. (2003). *Science*, **302**, 819–822.
- Greenamyre, J. T. & Hastings, T. G. (2004). *Science*, **304**, 1120–1122.
- Guldberg, H. C. & Marsden, C. A. (1975). *Pharmacol. Rev.* **27**, 135–206.
- Karhunen, T., Tilgmann, C., Ulmanen, I., Julkunen, I. & Panula, P. (1994). *J. Histochem. Cytochem.* **42**, 1079–1090.
- Lerner, C., Ruf, A., Gramlich, V., Masjost, B., Zurcher, G., Jakob-Roetne, R., Borroni, E. & Diederich, F. (2001). *Angew. Chem. Int. Ed. Engl.* **40**, 4040–4042.
- Lotta, T., Vidgren, J., Tilgmann, C., Ulmanen, I., Melen, K., Julkunen, I. & Taskinen, J. (1995). *Biochemistry*, **34**, 4202–4210.
- Lundstrom, K., Salminen, M., Jalanko, A., Savolainen, R. & Ulmanen, I. (1991). *DNA Cell Biol.* **10**, 181–189.
- Lundstrom, K., Tenhunen, J., Tilgmann, C., Karhunen, T., Panula, P. & Ulmanen, I. (1995). *Biochim. Biophys. Acta*, **1251**, 1–10.
- Mannisto, P. T. & Kaakkola, S. (1999). *Pharmacol. Rev.* **51**, 593–628.
- Mannisto, P. T., Kaakkola, S., Nissinen, E., Linden, I. B. & Pohto, P. (1988). *Life Sci.* **43**, 1465–1471.
- Masjost, B., Ballmer, P., Borroni, E., Zurcher, G., Winkler, F. K., Jakob-Roetne, R. & Diederich, F. (2000). *Chemistry*, **6**, 971–982.
- Matthews, B. W. (1968). *J. Mol. Biol.* **33**, 491–497.
- Navaza, J. (1994). *Acta Cryst.* **A50**, 157–163.
- Olanow, C. W. & Stocchi, F. (2004). *Neurology*, **62**, S72–S81.
- Otwinowski, Z. & Minor, W. (1997). *Methods Enzymol.* **276**, 307–326.
- Rodrigues, M. L., Archer, M., Bonifacio, M. J., Soares-da-Silva, P. & Carrondo, M. A. (2001). *Acta Cryst.* **D57**, 906–908.
- Roth, J. A. (1992). *Rev. Physiol. Biochem. Pharmacol.* **120**, 1–29.
- Tenhunen, J., Salminen, M., Jalanko, A., Ukkonen, S. & Ulmanen, I. (1993). *DNA Cell Biol.* **12**, 253–263.
- Vidgren, J. (1998). *Adv. Pharmacol.* **42**, 328–331.
- Vidgren, J., Ovaska, M., Tenhunen, J., Tilgmann, C. & Lotta, T. (1999). *S-Adenosylmethionine-Dependent Methyltransferases: Structures and Functions*, edited by X. Cheng & R. M. Blumenthal, pp. 55–91. Singapore: World Scientific Publishing.
- Vidgren, J., Svensson, L. A. & Liljas, A. (1994). *Nature (London)*, **368**, 354–358.
- Weiss, M. S. (2001). *J. Appl. Cryst.* **34**, 130–135.
- Zurcher, G., Colzi, A. & Da Prada, M. (1990). *J. Neural Transm. Suppl.* **32**, 375–380.